Selective rearrangement of Nd^{3+} centers in $LiNbO_3$ under ferroelectric domain inversion by electron beam writing

P. Molina, M. O. Ramírez, J. García Solé, and L. E. Bausá
Departamento de Física de Materiales, Universidad Autónoma de Madrid, Madrid 28049, Spain

B. J. García
Departamento de Física Aplicada, Universidad Autónoma de Madrid, Madrid 28049, Spain
(Received 25 February 2008; published 30 July 2008)

Different values of the electronic charge provided by a direct electron beam writing system have been used to produce polarization inverted domain regions in the micrometer range on Nd^{3+} optically activated $LiNbO_3$. The effect of the electronic charge on the Nd^{3+} center structure has been studied by means of low-temperature luminescence from Nd^{3+} ions. The axial crystal field acting on the Nd^{3+} centers has been analyzed through the $^4F_{3/2}$ energy-level splitting of the Nd^{3+} ions. From there we have determined the position of Nd^{3+} ions into the Li^+ octahedra for the different unequivalent centers in domains reversed with different electronic doses. The results show that the axial crystal field acting on the unequivalent Nd^{3+} centers can be selectively modified by means of the different doses applied to produce the inversion of the polarization. Moreover, a control of the discrete shifts suffered by the Nd^{3+} ions into the Li^+ octahedra after the inversion process can be carried out in the range 0–0.02 Å by selecting the type of Nd center to be shifted by means of the different electronic charge. The behavior of each Nd^{3+} center after the polarization inversion under different doses can be discriminated and the different nature, as well as the polar character of the Nd^{3+} centers, is clearly manifested.

DOI: 10.1103/PhysRevB.78.014114 PACS number(s): 77.84.−s, 42.70.Mp, 61.80.Fe, 78.30.−j

I. INTRODUCTION

The possibility of using the quasiphase matching technique for efficient multifrequency conversion processes by periodically alternating ferroelectric domain structures with opposite spontaneous polarization has generated an important effort in the engineering of devices for harmonic generation or for optical parametric oscillation.[1–3] In this sense, numerous techniques have been developed toward obtaining monodimensional or bidimensional ferroelectric domain inverted patterns in $LiNbO_3$ (Ref. 4) since this is one of the most extensively used ferroelectric crystals. Direct electron beam writing (EBW) has appeared as a promising technique for ferroelectric domain inversion in undoped samples.[5,6] The main advantages of this technique are the versatility in designing a variety of structures and the high spatial resolution, which is related to the nanometric size of the electron beam diameter. In addition, the EBW technique can lead to high quality nonlinear photonic devices without the use of previous masking processes required in other methods. Recently, the authors have successfully used EBW to produce the polarization inversion in Nd^{3+} doped $LiNbO_3$.[7,8] Since laser action has been demonstrated from this system,[9] this technique appears as a very promising one for designing multifunctional solid-state lasers based on periodically poled rare-earth doped $LiNbO_3$ nonlinear photonic crystals.

From the fundamental viewpoint the polarization inversion in a ferroelectric crystal requires a strong rearrangement of the lattice that could affect the crystal structure of the optically active centers. In this sense, understanding the switching behavior in the microscopic scale, as well as the role of defects, is nowadays a very active subject directly relevant to the development of devices based on microdomain structures.[10] In the case of $LiNbO_3$ crystals it is accepted that the domain inversion is consistent with the movement of Li^+ ions from their octahedrons to the free octahedrons in the lattice crossing the nearest oxygen triangles. Thus, the initial Li-Nb-vacancy sequence is turned to a vacancy-Nb-Li sequence.[11]

Considering that Nd^{3+} is the most widely laser ion used nowadays, it is of particular relevance to investigate the domain reversed structures in Nd^{3+} doped $LiNbO_3$ crystals, as well as to determine how the polarization inversion can affect the optical spectroscopy of the Nd^{3+} laser ions. At the same time, the Nd^{3+} optically active ions can act as a probe to reveal the possible effects of the polarization inversion on the host crystal lattice.

Previous work based on Rutherford backscattering spectrometry (RBS)/channeling showed that Nd^{3+} ions are located in Li^+ sites in the crystal lattice. Optical spectroscopy studies on single domain Nd^{3+} doped $LiNbO_3$ showed the clear presence of three nonequivalent polar Nd^{3+} centers in the $LiNbO_3$ host. Those centers took place as a consequence of the different local charge compensation mechanisms needed when Nd^{3+} ions are substituted for Li^+ cations in the crystal.[12]

Very recently, the authors have shown how the crystal field affecting each one of those three Nd^{3+} unequivalent centers was slightly modified when the polarization of the ferroelectric domain was inverted by means of EBW. This result was obtained by analyzing the slight spectroscopic changes observed when comparing original and inverted microdomain regions on a same $LiNbO_3$:Nd^{3+} sample. After the polarization inversion the splitting of the $^4F_{3/2}$ metastable level of Nd^{3+} decreased slightly for all those three Nd centers.[8]

In this work we have used different electronic doses provided by the electron beam to produce the microdomain in-

TABLE I. Electron beam irradiation parameters used in this work.

	Domain A	Domain B	Domain C	Domain O
Electron energy (keV)	25	25	25	Nonirradiated
Irradiation current (pA)	200	200	200	
Scanned area (μm^2)	10×10	10×10	10×10	
Exposure time (s)	75	115	155	
Total electronic charge (C)	2×10^{-8}	3×10^{-8}	4×10^{-8}	

verted regions in $LiNbO_3:Nd^{3+}$ crystals. The aim of this work has been to study the effect of the different doses on the different optically active Nd^{3+} centers and to investigate how the nature of each particular center could be affected in a different manner by the polarization inversion of the $LiNbO_3$ host crystal. Low-temperature high-resolution total site selective spectroscopy has been applied to determine the energy splitting of the $^4F_{3/2}$ state of each Nd^{3+} center for different irradiation doses. The experimental results indicate not only that a rearrangement of Nd^{3+} centers takes place but that this rearrangement can be made in a selective way: each Nd^{3+} center requires a different threshold electronic dose to effectively reverse its dipolar moment. Accordingly, the main message of our work is that by means of different electronic doses we demonstrate that it is possible to act selectively on the position of the different optically active ions into the Li^+ octahedra and hence to control their respective optical properties.

II. EXPERIMENT

A 650-μm-thick plate from a congruent single domain $Nd^{3+}:LiNbO_3$ crystal was cut and polished with its main faces oriented perpendicular to the ferroelectric *c* axis. Nd^{3+} concentration in the crystal was 0.1 wt %. Direct electron beam writing on the c^- face of the crystal was carried out by means of a Philips XL30 Schottky field-emission gun scanning electron microscope. Before the electron bombardment, a 100-nm thin film of Al was evaporated onto the c^+ face of the sample, which acted as a ground electrode during the electron beam bombardment. The main irradiation parameters were: 25 keV incident electron energy and 200 pA irradiation current. In order to facilitate the spectroscopic measurements, areas of around 100 μm^2 were irradiated to produce relatively large reversed domain structures. By using different exposure times, three different values of the total electronic charge were used to produce the polarization inverted microdomains: 2×10^{-8}, 3×10^{-8}, and 4×10^{-8} C. The irradiation parameters are summarized in Table I.

Total site selective spectroscopy (TSSS) was carried out at 10 K by using a liquid He cryostat well after the electronic irradiation processes. An Ar^+ pumped continuous-wave Ti:sapphire laser (Spectra Physics 3900) was used as a tunable excitation source. The beam of the Ti:sapphire laser was perpendicularly focused onto the center of different inverted regions on the c^+ face of the sample by means of a $100\times$ microscope objective. In this way, it has been possible to analyze and compare the spectra of Nd^{3+} ions coming from different microscopic ferroelectric domains. The emerging luminescence was collected with the same microscope objective and then directed into a double-grating monochromator. The detection was carried out with a liquid N_2 cooled charge coupled device detector. It is important to mention that a selective chemical etching (in a 2:1 solution of $HNO_3:HF$ at 60 °C for 20 min) was performed in order to reveal and confirm the effective domain inversion on the irradiated areas of the sample.

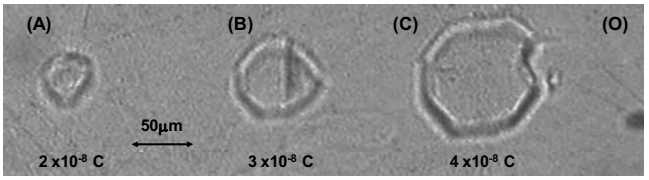

FIG. 1. Optical microphotograph showing ferroelectric domains in $LiNbO_3:Nd^{3+}$ obtained by EBW by means of different electronic doses. Values of the doses are indicated on the bottom of the photograph for each domain. (O) Original region; (A), (B), and (C) correspond to the domains inverted with doses of 2×10^{-8}, 3×10^{-8}, and 4×10^{-8} C, respectively.

III. RESULTS AND DISCUSION

The use of direct electron beam irradiation onto Nd^{3+} doped $LiNbO_3$ single domain crystals produced polarization inverted domain regions consisting of columns parallel to the ferroelectric *c* axis, traversing the whole sample thickness (650 μm), and with diameter sizes ranging from 10 to 100 μm. Figure 1 shows an optical microphotograph of the c^+ face of the sample after the direct electron beam writing process. As can be observed on Fig. 1, the final diameter sizes of the inverted region are related to the total electronic charge used to produce the polarization inversion; the higher the electronic dose, the bigger the diameter of the obtained inverted domain. This effect could be attributed to the effect of electronic repulsion and/or diffusion during the irradiation process, which spreads the electronic charge on a bigger area than the scanned region.

The good crystal quality and homogeneity of the domain inverted regions was confirmed by means of room-temperature micro-Raman spectra. In this respect, no differences were observed on the Raman spectra when comparing the original and inverted regions.[7]

The emission spectrum of Nd^{3+} ions in $LiNbO_3$ consists of several groups of lines corresponding to transitions from the $^4F_{3/2}$ metastable excited state to the different ^4I_J ($J=9/2$, 11/2, 13/2, and 15/2) terminal states of the $4f^3$ electronic configuration. According to previous works, Nd^{3+} ions are located into the Li^+ octahedra with a local symmetry

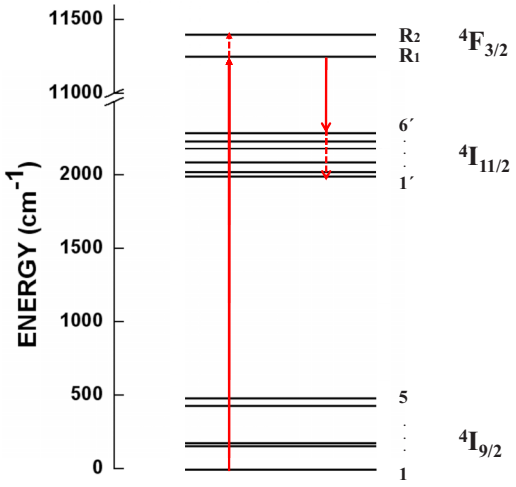

FIG. 2. (Color online) Simplified energy-level scheme of Nd^{3+} ions showing the relevant excitations: ${}^4I_{9/2} \rightarrow R_1, R_2$ and emission: $R_1 \rightarrow {}^4I_{11/2}$ transitions involved in our experiments.

C_3.[12,13] Under that symmetry the different states split into $(2J+1)/2$ doublet-Kramer levels. The two crystal-field components of the ${}^4F_{3/2}$ state were called R_1 and R_2, while the split components of the ${}^4I_J$ states were labeled by numbers 1, 2,… in order of increasing energy.

We have centered our experiments on the ${}^4F_{3/2}$ metastable excited state. This ${}^4F_{3/2}$ state splits into the two crystal-field levels, R_1 and R_2, only by deviations from the cubic symmetry. In the case of $LiNbO_3$ the amount of this splitting gives a measure of the axial distortion of the crystalline field around the emitting Nd^{3+} ions. Figure 2 shows a simplified energy-level scheme of the relevant Stark sublevels including the ${}^4I_{9/2} \rightarrow {}^4F_{3/2}$ (R_1 and R_2) excitations and the ${}^4F_{3/2}$ $(R_1) \rightarrow {}^4I_{11/2}$ emissions involved in our experiments.

Figure 3(a) shows the TSSS contour plot corresponding to the ${}^4I_{9/2}(1) \rightarrow R_1, R_2$ excitation region monitoring the $R_1 \rightarrow {}^4I_{11/2}(1')$ emission transition (at around 1082 nm). The

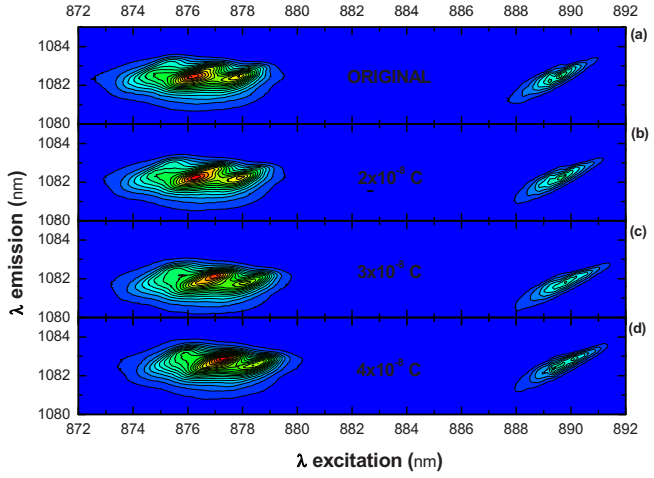

FIG. 3. (Color online) Low-temperature total site selective spectra of Nd^{3+} ions for four different regions studied, original (a) and inverted (b, c, and d). The excitation corresponds to the ${}^4I_{9/2} \rightarrow R_1, R_2$ transitions; the emission corresponds to the $R_1 \rightarrow {}^4I_{11/2}(1')$ transition.

presence of three major Nd^{3+} centers is clearly observed through the triplet structure on the ${}^4I_{9/2}(1) \rightarrow R_2$ excitation component. According to previous works these centers correspond to the so-called Nd-1, Nd-2, and Nd-3 centers present in $LiNbO_3:Nd^{3+}$ crystals.[13] The RBS/channeling together with spectroscopic results concluded that these Nd^{3+} centers are related to three different positions of the Nd^{3+} ions inside the Li^+ octahedron. These different positions consist of slight deviations of Nd^{3+} ions from the regular Li^+ sites along the ferroelectric c axis. Their origin can be associated with different charge compensation mechanisms needed when the trivalent Nd^{3+} ions substitute for the Li^+ ions into the host crystal. As has been suggested, these charge compensation mechanisms occur at the cost of different relative positions of the Li^+ vacancies with respect to the Nd^{3+} location, which would originate the shifts of Nd^{3+} along the c axis in their octahedrons and therefore the spectroscopic unequivalence of Nd^{3+} centers.[14–16]

By means of the study of the TSSS from the different ferroelectric domains it has been possible to analyze the behavior and the evolution of the structure of centers present in the $LiNbO_3:Nd^{3+}$ crystal after ferroelectric domain inversion using different electronic charge. Figures 3(b), 3(c), and 3(d) show the TSSS contour plots for the inverted ferroelectric domains A, B, and C depicted in Fig. 1. As can be noticed, the position of the emission/excitation peaks associated with the Nd-1, Nd-2, and Nd-3 centers is shifted with respect to those obtained from the original region depending on the value of the electronic charge used to produce the inversion. This significant result reveals that the electronic bombardment produces modifications of the Nd^{3+} centers, which depend on the electric field (electronic dose) producing the polarization inversion of the crystal.

In our experiments, the energy splitting of the ${}^4F_{3/2}$ state for each one of the three centers in the different ferroelectric domains of our sample have been obtained by a detailed analysis of the TSSS results, extracting the information corresponding to the ${}^4I_{9/2}(1) \rightarrow R_1, R_2$ excitations for each center in each domain (O, A, B, and C). In the original domain (O region) the values of the energy splitting are 144, 172, and 196 cm^{-1} for the Nd-1, Nd-2, and Nd-3 centers, respectively. The energy splitting values are modified after the inversion processes. Moreover, what is particularly relevant is that those values are selectively modified by the different charge dose used to reverse the polarization.

Figure 4 shows the changes in the energy splitting of the ${}^4F_{3/2}$ state for each center as a function of the electronic charge used to produce the polarization inversion. As can be seen the splitting of each center behaves in a different manner depending on the charge used to reverse the polarization. In domain A—obtained after inversion with the lowest charge 2×10^{-8} C—only the Nd-3 center is affected by lowering its splitting in 4 cm^{-1} relative to its value in the original noninverted region, while in the others Nd-1 and Nd-2 centers remain unaffected. For higher values of the electronic charge [3×10^{-8} C (domain B)], in addition to the change in the splitting of the Nd-3 center, a decrease of around 10 cm^{-1} is also observed in the energy splitting of the Nd-2 center—being now the Nd-1 center the only remaining unchanged. Finally, after inversion with the highest dose of 4

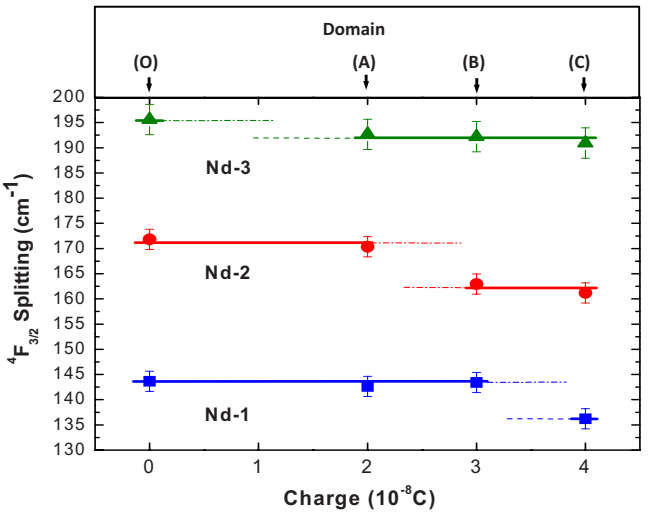

FIG. 4. (Color online) Energy splitting of the $^4F_{3/2}$ state for the three nonequivalent Nd^{3+} centers in the original (O) and inverted domains (A, B, and C).

$\times 10^{-8}$ C (domain C), the Nd-1 center is also affected by decreasing the energy splitting around 8 cm^{-1}. Thus, Fig. 4 shows that the Nd^{3+} centers are not simultaneously following the polarization inversion of the host crystal. The different nature of the centers is therefore manifested. Additionally, it is interesting to note that the more noncubic distortion of the Nd^{3+} environment (i.e., higher-energy splitting) the less charge is needed to modify the crystal field after the polarization inversion process.

A deeper analysis of the situation can be carried out by correlating the obtained value of the energy splitting of the $^4F_{3/2}$ state to the amount of the axial distortion, which is governed by the B_0^2 crystal-field parameter. By using Wybourne normalization, the energy splitting of the $^4F_{3/2}$ state, ΔE, is easily estimated as

$$\Delta E = 0.16 B_0^2. \tag{1}$$

In a simple overlap model (SOM) based on the ligand point-charge approximation this crystal-field parameter is given by[17,18]

$$B_0^2 = \rho\left(\frac{2}{1+\rho}\right)^3 \sum_j \frac{g_j}{\rho_j^3}\frac{1}{2}(3x_j^2 - 1)\langle r^2\rangle, \tag{2}$$

where ρ is the overlap coefficient for the Nd-O bonding, $g_j = 2$ is the number of electron ligand charges, ρ_j are the Nd^{3+} to O^{2-} distances in the Li^+ octahedron, $x_j = \cos\alpha_j$ is the cosine directors of the ligand ions, and $\langle r^2\rangle = 1.001 a_0^{-2}$ (a_0 being the Bohr radius) is the integral of the $4f$ Nd^{3+} radial function.[19] The advantage of using this simple model is that we can now estimate the location of Nd^{3+} ions along the c axis for each particular center. Thus, each Nd^{3+} center—with a specific value of the $^4F_{3/2}$ energy splitting—is related to a particular position of the Nd^{3+} ion inside the Li^+ octahedron.

Figure 5 shows in continuous line the theoretical dependence of the energy splitting of the $^4F_{3/2}$ state [by using the expressions (1) and (2)] as a function of the Nd^{3+} position along the c axis in the Li^+ octahedron. In the plot "x" is the

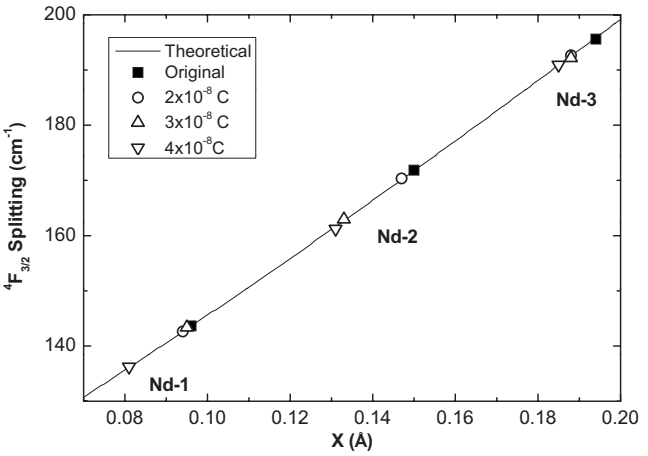

FIG. 5. Split of the $^4F_{3/2}$ state for the nonequivalent Nd^{3+} centers as a function of the position of Nd^{3+} ions along the c axis relative to the regular Li position into the Li octahedra.

shift relative to the regular Li^+ position (located at 0 Å). As observed, the value of the $^4F_{3/2}$ energy splitting increases with the shift relative to the regular Li^+ position. The values of ΔE obtained from our experimental results for the three Nd^{3+} centers in the original region (O region) are depicted in the figure as black squares. The results obtained after the inversion using different values of the electronic dose are shown as open symbols on the figure. As can be seen, after the polarization inversion the position of Nd^{3+} ions into the Li octahedra is slightly shifted toward the regular Li position. This fact is a consequence of the polarization inversion process occurring in the crystal. Moreover, the Nd^{3+} ions are not shifted simultaneously but they are altered depending on the electronic charge used in our experiments. For instance the Nd^{3+} ions in the Nd-1 center need a higher electronic charge to be shifted than those in the Nd-2 and Nd-3 centers. On the contrary, Nd^{3+} on the Nd-3 centers is shifted for all the electronic charge used in our experiments.

The results could be interpreted by considering the nonequivalent centers Nd-1, Nd-2, and Nd-3, such as polar defects, formed by the Nd^{3+} ions and their corresponding charge compensating Li^+ vacancies. Thus, different values of dipolar moments can be associated with each different center. In fact, polar defect pictures have been previously invoked to explain other ionic defect structures in $LiNbO_3$. In particular, polar defects involving Nb antisites in congruent $LiNbO_3$ crystals,[20,21] as well as polar defects related to RE^{3+} centers in $LiNbO_3$ crystals.[22,23]

According to our experiments each one of those polar Nd^{3+} centers would require a different threshold energy to reverse its dipolar moment. A schematic representation of the possible microscopic process is depicted in Fig. 6. As a starting point the original single domain crystal contains the three dipolar defects whose dipolar moments are pointing in the same sense than the macroscopic electric polarization vector of the lattice, Ps [Fig. 6(O)]. After electron beam writing with a charge of 2×10^{-8} C the macroscopic polarization of the crystal is locally inverted creating the domain A, region in gray color in the Fig. 6(A). For that electronic dose only the Nd-3 center is effectively reversed. At that stage the re-

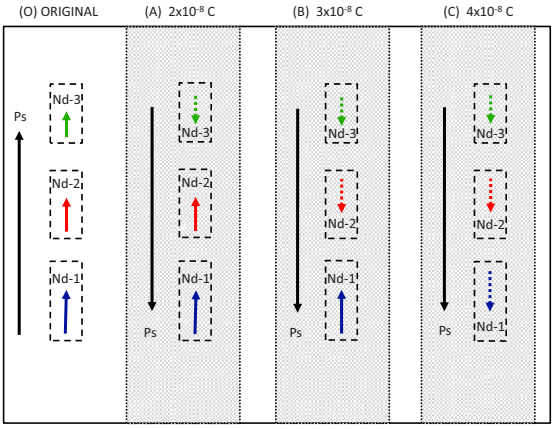

FIG. 6. (Color online) Qualitative schematics of selective reorientation of three polar Nd^{3+} centers under domain inversion of the host crystals with different electronic doses. Vectors in continuous line represent the dipolar moments of Nd^{3+} defects before rearrangement and those in dashed line after the rearrangement process. The modulus of vectors does not correspond to the quantitative contribution of the defects to the macroscopic polarization.

maining polar defects Nd-2 and Nd-1 still keep their dipolar moment antiparallel to the new orientation of the macroscopic polarization of the host crystal, constituting what has been called frustrated defect states.[20] When a higher electronic charge is used to invert the polarization of the crystal, a higher electric field is forcing those frustrated defects to reorient their dipolar moments in the same sense as that of the macroscopic polarization of the lattice Ps. Figure 6(B) represents the situation corresponding to the domain B after reversing the host with a charge value of 3×10^{-8} C. Now the Nd-2 defect is also affected, according to the experimental results of Fig. 4. Finally, when creating domain C—with a still higher charge (4×10^{-8} C)—the Nd-1 center is affected [see Fig. 6(C)]. By selecting the appropriate charge it is then possible to act selectively on the different polar Nd centers in the crystal. That is, it is possible to effectively reverse the dipole moment of each one of the Nd centers by irradiating with the appropriate electronic charge.

These results confirm that a rearrangement in the defect structure associated with the local environment of the Nd^{3+} ions and the Li^+ vacancy structure is taking place under the inversion process. In addition, our interpretation would confirm the presence of stable frustrated defects in ferroelectric crystal as previous authors have reported.[20]

What is clear from the optical spectroscopy is that upon domain reversal and upon a certain threshold of electronic dose Nd^{3+} ions slightly shift along the *c* axis inside the Li^+ octahedron but they keep inside the Li^+ octahedron. That is, Nd^{3+} ions are not following the movements of Li^+ ions (which cross the oxygen triangle toward the free octahedrons) they replace but they keep inside the Li^+ octahedron and slightly shift along the *c* axis relative to its previous position.[8]

At this moment it is important to take into account that the inversion of the spontaneous polarization direction does not give rise to an equivalent sequence of ions along the *c* axis. Although the initial Li-Nb-vacancy sequence is changed into a Vacancy-Nb-Li sequence, Nd^{3+} ions are keeping inside the Li^+ octahedrons—being responsible for the break of the equivalence between the two polarization states (up and down) and therefore responsible for the changes observed on the emission spectra.

The complexity of the process does not allow the determination of the exact mechanism affecting the Nd^{3+} environment and the possibility of the modification of the trapped charge located in the neighborhood of Nd^{3+} ions could be taken into account. If this would be the case, this trapped charge would only affect the percentage of Nd^{3+} ions in the crystal (0.1 wt %) since there is no evidence of other trapped charges in the matrix giving rise to any other additional types of defects in the crystals: neither the Raman spectra nor the optical spectroscopy on the whole VIS region show any change when comparing reversed domains by EBW.[7]

IV. SUMMARY

We have applied the versatile and direct technique of electron beam writing to produce bidimensional ferroelectric domain inversion patterning in Nd^{3+} doped $LiNbO_3$ crystals. By means of low-temperature high-resolution spectroscopy, it has been possible to determine the axial crystal field affecting the nonequivalent center structure for Nd^{3+} ions present in the original and inverted regions after ferroelectric domain inversion. Applying different electronic doses for domain reversing, it has been possible to reveal the role played by the defect structure on the ferroelectric inversion mechanism. We demonstrate that different threshold energy is required for each Nd^{3+} center to orient parallel to the spontaneous polarization of the matrix. As a consequence, it is then possible to act over the structure of centers to revert selectively the Nd^{3+} polar defects depending on the electronic charge. Moreover, we have shown that it is possible to control selectively the position of the different optically active ions into the Li^+ octahedra (by discrete shifts in the range 0–0.02 Å) and therefore it is possible to control their respective optical properties. The work constitutes an approach to understand the role of defects in the switching behavior in ferroelectric crystals and it has been performed on a very interesting crystal—in which laser action, as well as other non linear phenomena, has been demonstrated. The results of this work could be extended to other sensitive optically active ions whose optical properties could be spectrally and spatially modulated by the direct use of the versatile and powerful technique of EBW in the design of photonic structures.

ACKNOWLEDGMENT

This work has been supported by the Spanish Ministry of Education and Science under Contract No. MAT2007–64686.

[1] L. E. Myers, R. C. Eckardt, M. M. Fejer, R. L. Byer, W. R. Bosenberg, and J. W. Pierce, J. Opt. Soc. Am. B **12**, 2102 (1995).
[2] L. E. Myers and W. R. Bosenberg, IEEE J. Quantum Electron. **33**, 1663 (1997).
[3] R. L. Byer, J. Nonlinear Opt. Phys. Mater. **6**, 549 (1997).
[4] M. Houé and P. D. Townsend, J. Phys. D **28**, 1747 (1995).
[5] J. He, S. H. Tang, Y. Q. Qin, P. Dong, H. Z. Zhang, C. H. Kang, W. X. Sun, and Z. X. Shen, J. Appl. Phys. **93**, 9943 (2003).
[6] Y. Glickman, E. Winebrand, A. Arie, and G. Rosenman, Appl. Phys. Lett. **88**, 011103 (2006).
[7] P. Molina, B. J. García, F. Agulló-Rueda, M. O. Ramírez, and L. E. Bausá, Ferroelectrics **343**, 334 (2006).
[8] P. Molina, D. Sarkar, M. O. Ramírez, J. García Solé, L. E. Bausá, B. J. García, and J. E. Muñoz Santiuste, Appl. Phys. Lett. **90**, 141901 (2007).
[9] T. Y. Fan, A. Cordova-Plaza, M. J. F. Digonnet, R. L. Byer, and H. J. Shaw, J. Opt. Soc. Am. B **3**, 140 (1986).
[10] S. Jesse, B. J. Rodriguez, S. Choudhury, A. P. Baddorf, I. Vrejoiu, D. Hesse, M. Alexe, E. A. Eliseev, A. N. Morozovska, J. Zhang, L. Chen, and S. V. Kalinin, Nat. Mater. **7**, 209 (2008).
[11] P. W. Haycock and P. D. Townsend, Appl. Phys. Lett. **48**, 698 (1986).
[12] J. García Solé, A. Lorenzo, T. Petit, G. Boulon, B. Roux, and H. Jaffrezic, J. Phys. IV **4**, C4-293 (1994).
[13] H. Loro, M. Voda, F. Jaque, J. García Solé, and J. E. Muñoz Santiuste, J. Appl. Phys. **77**, 5929 (1995).
[14] A. Lorenzo, H. Jaffrezic, B. Roux, G. Boulon, and J. García Solé, Appl. Phys. Lett. **67**, 3735 (1995).
[15] J. Solé, T. Petit, H. Jafrezic, and G. Boulon, Europhys. Lett. **24**, 719 (1993).
[16] A. Lorenzo, H. Loro, J. E. Muñoz Santiuste, M. C. Terrile, G. Boulon, L. E. Bausá, and J. García Solé, Opt. Mater. (Amsterdam, Neth.) **8**, 55 (1997).
[17] O. L. Malta, Chem. Phys. Lett. **88**, 353 (1982).
[18] M. Faucher and P. Caro, J. Chem. Phys. **63**, 446 (1975).
[19] A. J. Freeman and R. E. Watson, Phys. Rev. **127**, 2058 (1962).
[20] S. Kim, V. Gopalan, K. Kitamura, and Y. Furukawa, J. Appl. Phys. **90**, 2949 (2001).
[21] V. Gopalan, V. Dierolf, and D. A. Scrymgeour, Annu. Rev. Mater. Res. **37**, 449 (2007).
[22] J. García Solé, L. E. Bausá, D. Jaque, E. Montoya, H. Murrieta, and F. Jaque, Spectrochim. Acta, Part A **54**, 1571 (1998).
[23] V. Dierolf, C. Sandmann, V. Gopalan, S. Kim, and K. Polgar, Radiat. Eff. Defects Solids **158**, 247 (2003).